Journal of Hydrology 397 (2011) 238–249

Contents lists available at ScienceDirect

Journal of Hydrology

journal homepage: www.elsevier.com/locate/jhydrol

Sensitivity analysis of unsaturated flow and contaminant transport with correlated parameters

Feng Pan [a,d,*], Jianting Zhu [b], Ming Ye [c], Yakov A. Pachepsky [a], Yu-Shu Wu [e]

[a] USDA-ARS Environmental Microbial & Food Safety Lab, 10300 Baltimore Ave., BARC-EAST Bldg. 173, Beltsville, MD 20705, USA
[b] Division of Hydrologic Sciences, Desert Research Institute, Nevada System of Higher Education, Las Vegas, NV 89119, USA
[c] Department of Scientific Computing, Florida State University, Tallahassee, FL 32306, USA
[d] Department of Environmental Science & Technology, University of Maryland, College Park, MD 20742, USA
[e] Department of Petroleum Engineering, Colorado School of Mines, Golden, CO 80401, USA

ARTICLE INFO

Article history:
Received 10 June 2010
Received in revised form 7 October 2010
Accepted 30 November 2010
Available online 4 December 2010

This manuscript was handled by A. Bardossy, Editor-in-Chief, with the assistance of Purna Chandra Nayak, Associate Editor

Keywords:
Sensitivity analysis
Uncertainty analysis
Unsaturated flow
Contaminant transport
Parameter correlation

SUMMARY

This study conducts sensitivity and uncertainty analysis for predicting unsaturated flow and contaminant transport in a layered heterogeneous system. The objectives of this work are to: (1) examine the effects of parameter correlations on the sensitivity of unsaturated flow and contaminant transport and (2) assess the relative contributions of parameter uncertainties to the uncertainties of flow and transport at each hydrogeologic layer. Using the unsaturated zone (UZ) of Yucca Mountain (YM) in Nevada, USA, as an example, the study considers cases of independent and correlated parameters. A sampling-based regression method is used, when the model input parameters are independent, and a decomposition method is used for the correlated case. When the parameters are independent, the uncertainty in permeability has the largest contribution to the uncertainties in simulated percolation flux and mass of the reactive tracer arriving at the water table. For the percolation flux, the second largest contribution is from the van Genuchten α; the sorption coefficient of the reactive tracer is the second most important parameter for the tracer mass arrival uncertainty. The sensitivity to the sorption coefficient is larger in the layers of devitrified and zeolitic tuffs than in the layers of vitric tuff. Contributions of the uncertainties in van Genuchten n and porosity to the percolation flux and tracer transport uncertainties are larger in the case of correlated parameters compared with the case of independent parameters due to the correlations of n and porosity with the van Genuchten α and permeability, respectively. These results illustrate the significant effects of parameter correlations on the sensitivity and uncertainty of unsaturated flow and transport. The findings are of significance in facilitating future characterizations to reduce the parameter uncertainties and associated predictive uncertainties of flow and contaminant transport in unsaturated fractured porous media.

1. Introduction

Sensitivity analysis of flow and contaminant transport in unsaturated zone (UZ) is important for water resources management, environmental regulation, and remediation design. In general, it quantifies variation in outputs of unsaturated flow and transport models due to changes in model input parameters or other model components, such as boundary conditions or model structures. The input parameters are usually treated as random variables due to the epistemic uncertainties (spatial variability without sufficient characterization) and lack of measurements or knowledge. A common practice is to conduct uncertainty analysis (e.g., through stochastic modeling) for estimating probability distribution (or its leading moments) of the quantities of interest. Sensitivity analysis is always conducted together with the uncertainty analysis, and one purpose of the sensitivity analysis is to determine contributions of uncertainties in individual input parameters to predictive uncertainties in quantities of interest from flow and contaminant transport modeling.

The correlations among hydraulic parameters have important effects on the estimation of hydraulic parameters and further significantly affect the predictions and associated uncertainties of flow and tracer transport (Pohlmann et al., 2002; Lemke et al., 2004; Manache and Melching, 2008). Although the parameter correlations are observed and may be strong in some cases, existing sensitivity analysis methods of unsaturated flow and transport typically adopt the assumption of independent parameters (e.g., Li and Yeh, 1998; Boateng and Cawlfield, 1999; Boateng, 2007; Zhu et al., 2010). Only a few studies have been devoted to the

* Corresponding author at: USDA-ARS Environmental Microbial & Food Safety Lab, 10300 Baltimore Ave., BARC-EAST Bldg. 173, Beltsville, MD 20705, USA. Tel.: +1 301 504 6443; fax: +1 301 504 6608.
E-mail address: feng.pan@ars.usda.gov (F. Pan).

0022-1694/$ - see front matter © 2010 Elsevier B.V. All rights reserved.
doi:10.1016/j.jhydrol.2010.11.045

sensitivity analysis with correlated input parameters (Helton et al., 1995; Fang et al., 2004; Jacques et al., 2006). Understanding the contribution of each parameter and joint contributions of correlated parameters in predictive uncertainties is also critical to uncertainty reduction (Rojas et al., 2009; Fox et al., 2010).

The sensitivity analysis answers the question of how the outputs depend on the uncertain inputs (e.g., Jacques et al., 2006). Local sensitivity analysis evaluates how the outputs change by varying one input parameter at a time. Global sensitivity analysis assesses how the output uncertainties are related to the uncertainties of input parameters with all the variation range of inputs (Jacques et al., 2006). This study is focused on the global sensitivity analysis. Widely used sensitivity analysis methods include sampling-based method (Helton, 1993; Helton and Davis, 2002; Helton et al., 2005, 2006), screening method (Morris, 1991; Campolongo et al., 2007; Muñoz-Carpena et al., 2007; Fox et al., 2010), variance-based method such as the Fourier Amplitude Sensitivity Test (FAST) (Cukier et al., 1973, 1978; Sobol, 1993; Saltelli et al., 1999, 2008; Lu and Mohanty, 2001; Muñoz-Carpena et al., 2010), analysis of variance (ANOVA) (McKay, 1997; Sobol, 2001; Winter et al., 2006), and classification tree technique (Mishra et al., 2003; Mishra, 2009). Among them, the sampling-based (i.e., Monte Carlo) methods have been widely applied for global sensitivity analysis. The method is conceptually simple and able to cover the full range of parameter uncertainties. More importantly, the method allows one to directly obtain predictive uncertainty results without using surrogate models (e.g., Taylor series approximation, response surface approximation, and Fourier series) to represent the original model; mapping relations between uncertainty inputs and analysis results can be easily established (Helton, 1993). Because the sampling-based method employs linear regression techniques, the rank transformation is often a preferred way when the relationship between the parameter inputs and analysis results is nonlinear (Saltelli and Sobol, 1995). For the sampling-based method, the sensitivity measure, standardized rank regression coefficient (SRRC), is a robust and reliable estimator (e.g., Saltelli and Marivoet, 1990; Helton and Davis, 2002). When the input parameters are correlated, however, SRRC may give unreliable results on estimation of parameter importance (Helton et al., 2006). Recently, Xu and Gertner (2008) proposed a decomposition method to separate the contributions of individual parameter uncertainties to the output uncertainties into the correlated and uncorrelated parts, which is adopted in this study.

The UZ of Yucca Mountain (YM), Nevada, once considered as the potential high-level radioactive waste repository, is used as the study site. The UZ of YM is a complex system of distinct hydrogeologic layers with significant parameter uncertainties (Zhou et al., 2003; BSC, 2004a; Wu et al., 2004, 2007; Illman and Hughson, 2005; Zhang et al., 2006; Ye et al., 2007; Pan et al., 2009a,b). The available measurements of hydraulic parameters are limited in each hydrogeologic layer of the UZ, especially for permeability and water retention parameters. The results of sensitivity analysis can be particularly helpful in targeting future measurements to the most influential parameters in the particular layers to better utilize limited resources for reducing predictive uncertainties in flow and contaminant transport. The sensitivity of the flow and tracer transport at YM has been investigated by several studies (Lu and Mohanty, 2001; Mohanty and Wu, 2001; Mishra et al., 2003; Zhang et al., 2006). Zhang et al. (2006) examined the sensitivity of unsaturated flow and tracer transport by varying only one input parameter at a time within one standard deviation. The most influential parameters of total-system performance assessment at YM were identified by FAST, cumulative distribution function (CDF)-based method, and classification tree technique (Lu and Mohanty, 2001; Mohanty and Wu, 2001; Mishra et al., 2003). These previous studies, however, have not addressed the layer-scale sensitivity, and the effects of parameter correlations have been largely omitted. The objective of this study is to evaluate and compare contributions of uncertainties in individual input parameters to flow and contaminant transport uncertainties with and without parameter correlations at the layer-scale in the unsaturated zone.

2. Materials and methods

2.1. Study site

The UZ of YM is between 500 and 700 m thick and is a complex geologic formation that includes heterogeneous layers and anisotropic fractured tuffs (Montazer and Wilson, 1984). The UZ consists of five major geologic units: Tiva Canyon welded (TCw) unit, Paintbrush nonwelded (PTn) unit, Topopah Spring welded (TSw) unit, Calico Hills nonwelded (CHn) unit, and Crater Flat undifferentiated (CFu) unit (Fig. 1). Each unit is further divided into multiple hydrogeologic layers, resulting in 33 layers. The three-dimensional (3-D) UZ model has been developed to simulate various physical processes in the UZ of YM (BSC, 2004a; Wu et al., 2004). The unsaturated flow module, EOS9, and radionuclide transport module, T2R3D, of the TOUGH2-family (Wu et al., 1996; Pruess et al., 1999) are applied for simulating the unsaturated flow and tracer transport. The details of the conceptual model, numerical model, model domain, site measurements and variations of the parameters are given in Appendix A. In this study, the model input parameters (e.g., porosity, permeability, van Genuchten α and n, and sorption coefficient of reactive tracer) are treated as random variables to assess the uncertainty and sensitivity of unsaturated flow and tracer transport. The random model parameters are generated based on the site measurements and statistical methods.

2.2. Sampling-based regression method and decomposition method

The sampling-based regression method and decomposition method are used for the sensitivity analysis with independent and correlated model parameters, respectively. The sampling-based method is implemented in the following procedures (Helton, 1993; Helton et al., 2005):

(1) Determine the probability distributions and ranges of individual parameters based on the field measurements.
(2) Generate multiple realizations of random parameters based on the estimated distributions and ranges.
(3) Solve the flow and transport problems for each realization.
(4) Evaluate uncertainties of the output variables (e.g., saturation, water potential, percolation flux, mass fraction and travel time of tracer transport).
(5) Conduct the sensitivity analysis to rank the relative importance of the individual parameters to the uncertainties of output variables.

The sensitivity analysis (i.e., step 5) is first carried out based on the Monte Carlo simulation results of Ye et al. (2007) and Pan et al. (2009b), in which the correlations between permeability and porosity and between van Genuchten α and n are considered. In order to evaluate the effects of parameter correlations, uncorrelated parameters are generated and additional Monte Carlo simulations are carried out in this study.

The regression model relating the model outputs (e.g., percolation flux and cumulative mass arrival) and the input parameters (i.e., permeability, porosity, van Genuchten α and n, and sorption coefficient of the reactive tracer in this study) is constructed for each numerical gridblock as (Helton, 1993; Helton and Davis, 2002; Helton et al., 2006)

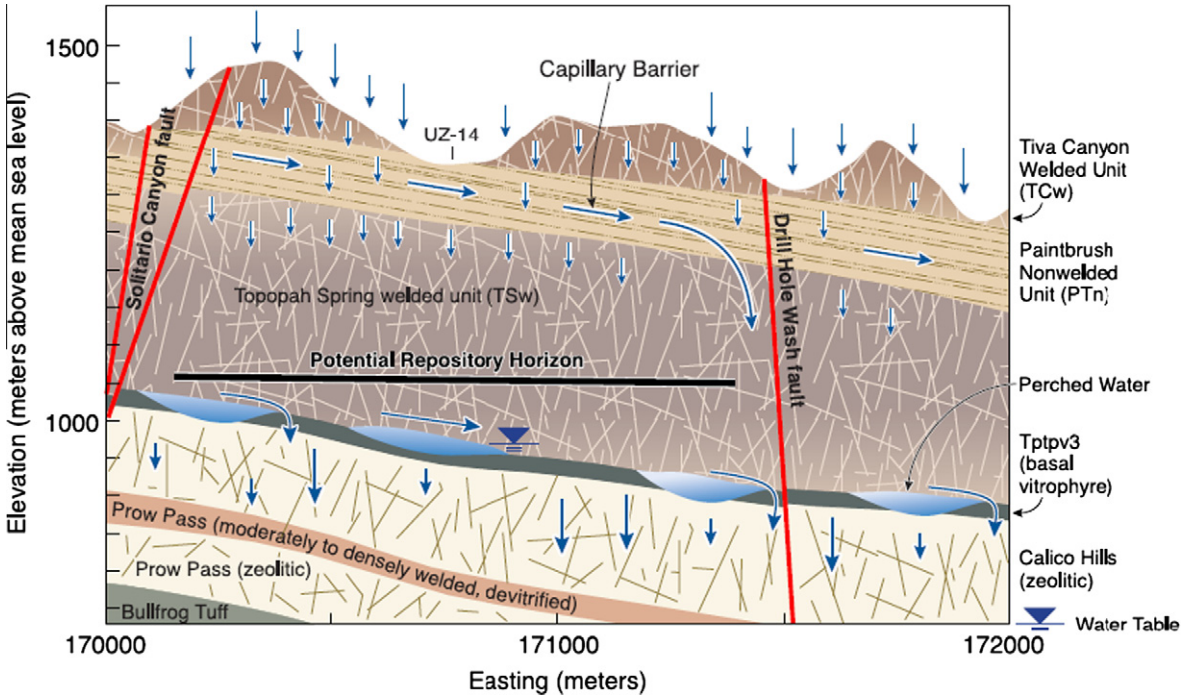

Fig. 1. Schematic illustration of the conceptualized flow processes and effects of capillary barriers, major faults, and perched-water zones within a typical east–west cross section of the UZ flow model domain (modified from BSC, 2004a).

$$\hat{y}_i = b_0 + \sum_j b_j x_{ij}, \quad i = 1, 2, \ldots, m, \;\; j = 1, 2, \ldots k \tag{1}$$

where m is number of realizations (m = 200 in this study), k is number of input parameters (k = 5 in this study), $\hat{y}_i$ is the estimation of output y_i by the regression model, x_{ij} is the ith realization of the jth model input parameter, b_0 is a regression coefficient, and b_j is regression coefficients for parameter j. Due to the different units of input parameters and outputs, b_j cannot be used to directly measure the parameter importance. This problem is resolved by standardizing the regression model (Eq. (1)), which leads to the following normalized equation,

$$(\hat{y}_i - \bar{y})/\hat{s} = \sum_{j=1}^{k} (b_j \hat{s}_j/\hat{s})(x_{ij} - \bar{x}_j)/\hat{s}_j \quad i = 1, 2, \ldots m \tag{2}$$

where $\bar{x}_j$ and $\hat{s}_j$ are mean and standard deviation of the input parameter x_{ij}, respectively, and $\bar{y}$ and $\hat{s}$ are mean and standard deviation of the output y_i. The coefficient $b_j\hat{s}_j/\hat{s}$ is the standardized regression coefficient (SRC), used to measure the contribution from parameter j to the output variable uncertainty. In other words, parameters with larger |SRC| values contribute more to the output uncertainties.

The regression model is based on the linear relationships between the input parameters and the outputs. If the relationships are nonlinear, which is typical for complex models such as in this study, the linear regression may not provide accurate estimations. The problem can be alleviated by using the rank regression that is similar to the regression analysis (Saltelli and Sobol, 1995). The only difference is that the input and output data used in the usual regression model are transformed to their corresponding ranks. The smallest value of each variable of input and output data is ranked No. 1, the next larger value No. 2, and so on. Note that the ranking rules are consistent for the inputs and outputs. The contribution of each variable is measured by the square or absolute values of its regression coefficients. Correspondingly, the resulting regression coefficients are called the standardized rank regression coefficients (SRRC).

For each computational gridblock, the total variance (V) of the output over the m realizations is calculated via

$$V = \mathrm{var}(y) = \frac{1}{m-1}\sum_{i=1}^{m}(y_i - \bar{y})^2 \tag{3}$$

For the same gridblock, the variance ($\hat{V}$) of the regression estimated output is

$$\hat{V} = \mathrm{var}(\hat{y}) = \frac{1}{m-1}\sum_{i=1}^{m}(\hat{y}_i - \bar{y})^2 \tag{4}$$

The extent to what the regression model can account for the output uncertainty is measured by the coefficient of determination (R^2) (Helton, 1993; Saltelli et al., 2000; Helton et al., 2006)

$$R^2 = \frac{\hat{V}}{V} \tag{5}$$

If the input parameters are independent, $\hat{V}$ can be calculated by taking the variance on both sides of Eq. (1), which leads to

$$\hat{V} = \mathrm{var}(\hat{y}) = \sum_{j=1}^{k} b_j^2 \mathrm{var}(x_j) \tag{6}$$

Considering Eqs. (2), (5), and (6) leads to

$$R^2 = \sum_{j=1}^{k} SRC_j^2 \tag{7}$$

The SRC^2 (or $SRRC^2$) represents the contribution proportion from individual input parameters to the uncertainties of output variables. In deriving Eq. (6), the correlation terms among the input parameters are omitted. As a result, when the input parameters are correlated, the SRC^2 (or $SRRC^2$) may not give true indications in terms of the parameter importance in output uncertainty (e.g., Saltelli et al., 2000; Helton et al., 2006). Xu and Gertner (2008)

developed an approach to decompose the output variance into the partial variance contributed by the correlated and uncorrelated portions of the input parameters. Since the method is also based on the linear relationships between the input parameters and the output variables, the rank transformation is also applied to alleviate the limitation of linear relationships. When the parameter correlation is considered, the regression model between the input parameters and outputs is constructed the same way as Eq. (1). The partial variance (V_j) of output variable contributed by parameter x_j is separated into the partial variances contributed by uncorrelated and correlated variances of parameter x_j, respectively, as follows:

$$V_j = V_j^U + V_j^C \tag{8}$$

where V_j^U is the partial variance contributed by the uncorrelated variance of parameter x_j, and V_j^C is the partial variance contributed by x_j correlated with other parameters. The partial variance of y contributed by x_j is estimated by the regression analysis:

$$\hat{y}_i^{(j)} = \theta_0 + \theta_j x_{ij}, \quad i = 1,2,\ldots m \text{ and } \hat{V}_j = \frac{1}{m-1}\sum_{i=1}^{m}(\hat{y}_i^{(j)} - \bar{y})^2 \tag{9}$$

where $\hat{y}_i^{(j)}$ is the regression estimation of output y_i by Eq. (9), θ_0 is regression coefficient, and θ_j is regression coefficients of parameter j.

The partial variance contributed by the uncorrelated variance of x_j can be derived from the following regression models:

$$\hat{y}_i^{(-j)} = r_0 + r_j \hat{z}_{ij} \quad i = 1,2,\ldots m \text{ and } \hat{V}_j^U = \frac{1}{m-1}\sum_{i=1}^{m}(\hat{y}_i^{(-j)} - \bar{y})^2 \tag{10}$$

where $\hat{z}_{ij} = x_{ij} - \hat{x}_{ij}$, $\hat{x}_{ij} = c_0 + \sum_{\substack{p=1 \\ p\neq j}}^{k} c_p x_{ip}$, and $\hat{y}_i^{(-j)}$ is the regression estimation of output y_i by Eq. (10), r_0, r_j, c_0, and c_p are regression coefficients. V_j^C can be calculated via Eq. (8). The sensitivity indices (ratios of partial variance and total variance, V) of each parameter can be described as:

$$S_j = \frac{\hat{V}_j}{V}; \quad S_j^U = \frac{\hat{V}_j^U}{V}; \quad S_j^C = \frac{\hat{V}_j^C}{V} \tag{11}$$

where S_j, S_j^U, and S_j^C are the total, uncorrelated, and correlated partial sensitivity indices of parameter x_j, respectively. The total sensitivity index, S_j, is used to measure the relative contributions of input parameter, x_j, to the flow and tracer transport uncertainties. The correlated sensitivity index, S_j^C, is specifically used to quantify the uncertainty contributions from x_j due to its correlations with the other parameters. The larger $|S_j|$ values indicate more significant sensitivity to the parameter j.

3. Results and discussion

The sensitivity coefficients (i.e., $SRRC^2$ for the independent parameters and the sensitivity indices S for the correlated parameters) are determined for each gridblock. Their mean values over all gridblocks within a layer are calculated as the measure of parameter importance to the flow and transport uncertainties, and their standard deviations are used to measure the variations of sensitivity coefficients within a layer.

3.1. Sensitivity analysis of unsaturated flow with independent and correlated parameters

The R^2 values are first used to examine reliability of the regression analysis. If R^2 value is larger than 0.7, the linear regression model is acceptable for the sensitivity analysis (Saltelli et al., 2006; Manache and Melching, 2008). The R^2 values in this study are larger than 0.8 in more than 80% gridblocks of the domain (e.g., Fig. 3d), indicating that the regression analysis is generally reliable.

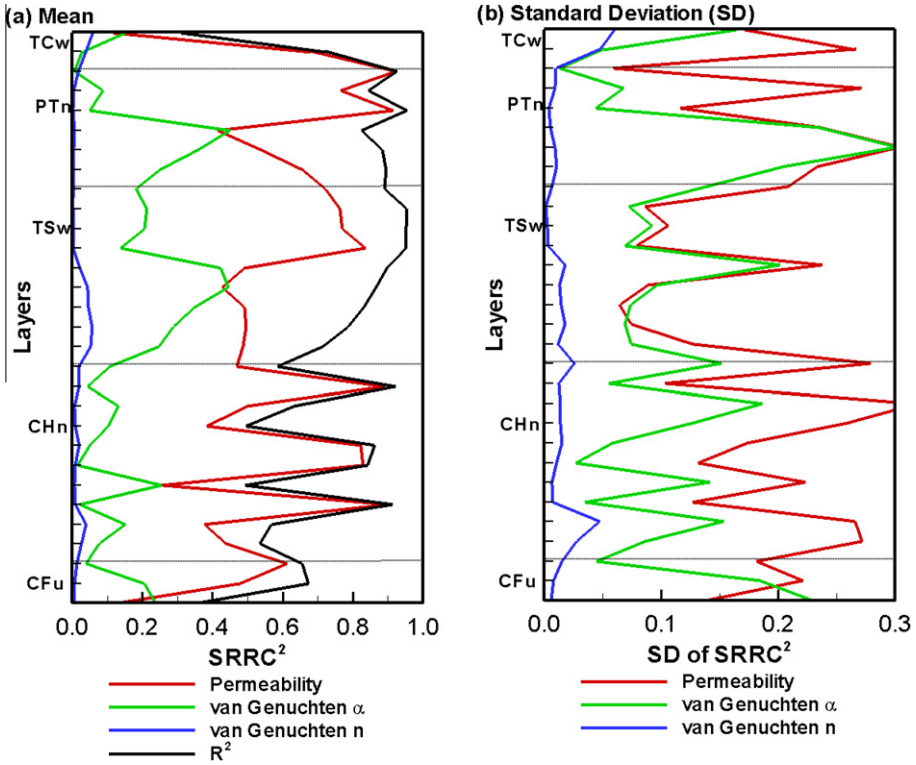

Fig. 2. The mean and standard deviation (SD) of standardized rank regression coefficent ($SRRC^2$) of permeability, van Genuchten α, and n parameters on percolation flux uncertainty at each layer (R^2 is the coefficient of determination value).

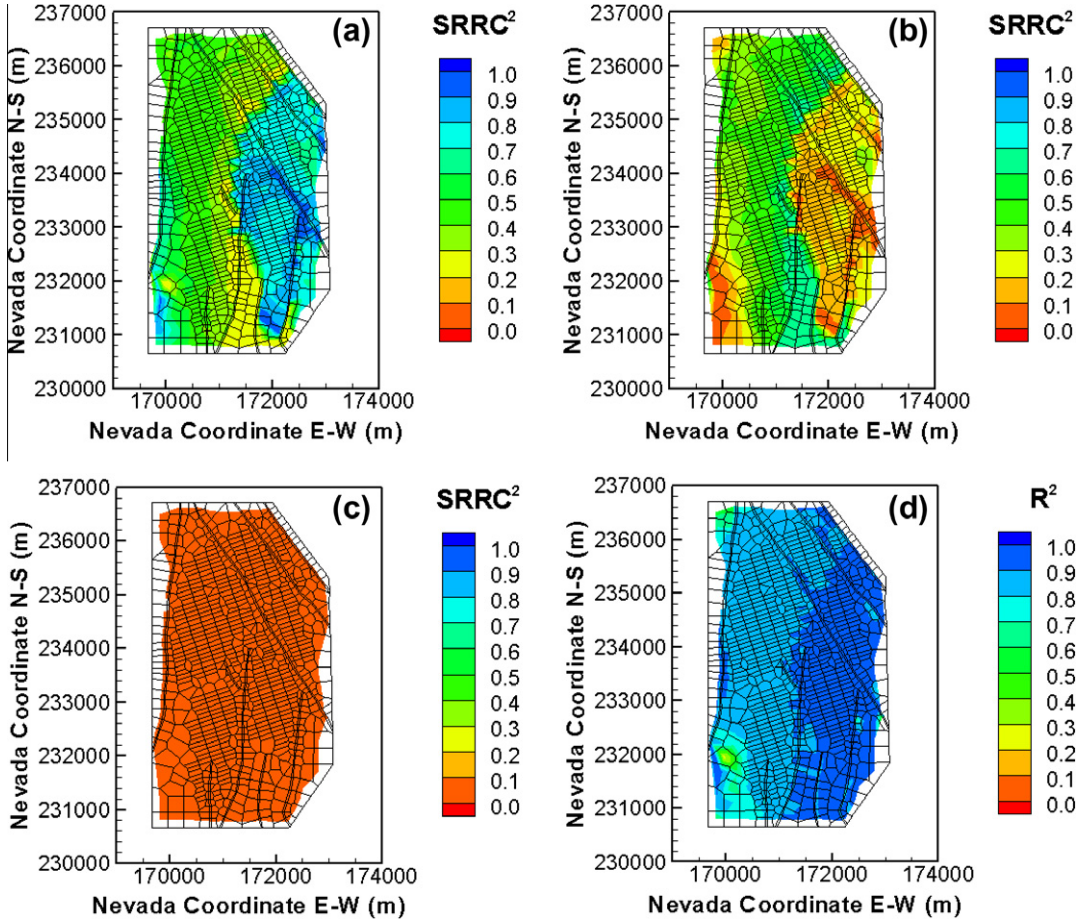

Fig. 3. The standardized rank regression coefficient (SRRC^2) of permeability (a), van Genuchten α (b) and n (c) parameters on percolation flux uncertainty and the coefficient of determination (R^2) values of regression analysis (d) at the tracer-releasing horizon (about 300 m below surface).

For the case of independent parameters, Fig. 2 plots the mean and standard deviation of SRRC^2 for the permeability, and van Genuchten α and n for the percolation flux for each hydrogeologic layer. The SRRC^2 value for a parameter represents the relative fractional contribution to the output variance from uncertainty in this parameter. Note that the summation of the SRRC^2 values for the three parameters is equal to the R^2 value, which validates Eq. (7). Among the three parameters affecting the unsaturated flow, the mean SRRC^2 values for the permeability are the largest for most layers, indicating that the parameter uncertainty in permeability has the largest contribution to the percolation flux uncertainty. The contributions of parameter uncertainty in permeability to the flux uncertainty vary with the layers from 20% to 80%. The mean SRRC^2 values of van Genuchten α are the second largest in most layers in the range of 0–40% contributions. The mean of SRRC^2 for van Genuchten n parameter is close to zero for all layers, indicative of the limited contributions of its uncertainty to the flux uncertainty. The general order of parameter importance to flux uncertainty, from the most to least important parameters, is permeability, van Genchten α and n for most layers, which is generally in line with the variances of these input parameters. Since the perched water may occur with the low-permeability zeolites in the CHn unit and the bottom of TSw unit in the UZ (Fig. 1), the fully saturated situations in the layers are checked. It is found that only very small percentage of gridblocks in the layers PV2a and CHZ are fully saturated. In this regard, the van Genuchten parameters are considered to be important in the layers. Fig. 2b shows the standard deviation of SRRC^2 is large for permeability and van Genuchten α for most layers, which indicates the large spatial variation of the sensitivity of the two parameters to flux uncertainty within each layer.

Since percolation flux uncertainty in a computational gridblock is related not only to the parameter uncertainty at the gridblock but also to the parameters at other locations, especially those above the gridblock, it is necessary to investigate the spatial distribution of the sensitivity coefficients within each layer. Fig. 3 depicts the spatial distribution of SRRC^2 values for the permeability and van Genuchten α and n as well as the R^2 values of regression analysis at the tracer-releasing horizon about 300 m below the surface. The large R^2 values (Fig. 3d) indicate reliable regression analysis in general. The SRRC^2 values for the permeability are the largest in most parts of layer; the values are approximately equal to or slightly smaller than those for the van Genuchten α in the tracer-releasing area (blue dots in Fig. A.1). The SRRC^2 values of van Genuchten n are close to zero in the entire domain. The degree of spatial variability of SRRC^2 values is similar for the permeability and van Genuchten α. These findings are consistent with the results of layer-scale shown in Fig. 2.

For the case of correlated parameters, the total, uncorrelated, and correlated sensitivity indices, S, are calculated to measure the contributions of input parameter uncertainty to the output uncertainty. As mentioned earlier, two pairs of correlated parameters are considered: (1) permeability and porosity and (2) van Genuchten α and n. Due to paucity of measurements, the correlations among other parameters are not considered. The Spearman rank correlations of the two pairs of parameters are listed in Tables A.1 and A.2 for each hydrogeologic layer.

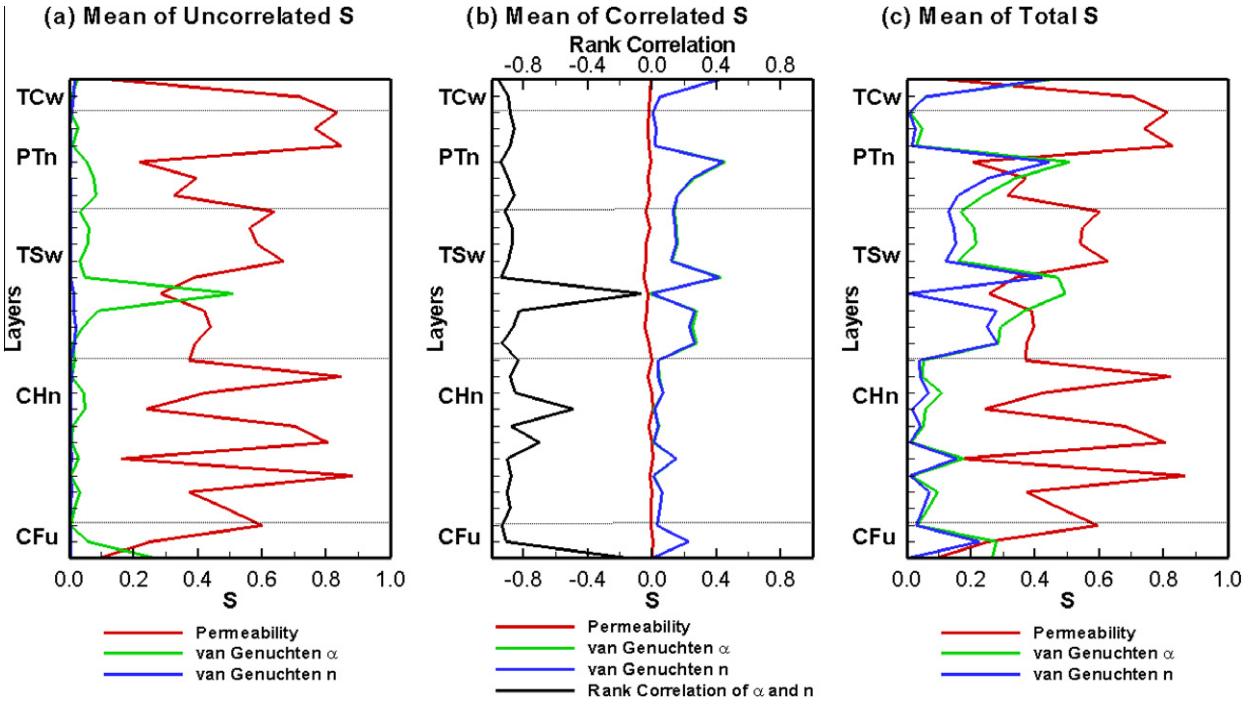

Fig. 4. The sensitivity indices (S) of permeability, van Genuchten α, and n parameters for each layer. (a) mean of uncorrelated S; (b) mean of correlated S; and (c) mean of total S.

Fig. 4 plots the mean values of the uncorrelated, correlated, and total S for the three parameters for each layer. As shown in Fig. 4a, the partial variance contributed by uncorrelated variance of permeability is dominant for all the layers, while the uncorrelated variance of van Genuchten n is close to zero for the layers. The mean values of the correlated S (Fig. 4b) for the van Genuchten α and n are almost identical due to the strong correlation between these two parameters. The mean values of the correlated S for permeability are close to zero for the layers, because the permeability is uncorrelated with the van Gencuten α or n parameters (the correlation between permeability and porosity does not appear to affect the flow uncertainty). The mean total S (Fig. 4c) is used to rank the relative importance of parameter uncertainty to the flux uncertainty when the input parameters are correlated. Fig. 4c shows the permeability is still the most important parameter for most layers; the van Genuchten n has more contributions to the flux uncertainty in several layers, indicative of increased contributions of van Genuchten n to the predictive uncertainty due to the correlation between n and α.

In addition to the correlated S values, Fig. 4b also plots, in solid line, the correlations between van Genuchten α and n for all layers. The mean values of correlated S for van Genuchten α and n have the same trend as the absolute correlations, suggesting that the partial variances contributed by the correlated input parameters largely depends on their correlations. For the permeability, the mean values of $SRRC^2$ (Fig. 2a) are larger than those of the total S (Fig. 4c) in most layers, while the opposite is true for the van Genuchten n. This indicates that the importance of permeability decreases while that of van Genuchten n increases, because the parameter correlations are considered.

3.2. Sensitivity of contaminant transport with independent and correlated parameters

Two variables are of particular importance to contaminant transport sensitivity: normalized cumulative mass arrival at each gridblock and cumulative mass travel time. The normalized cumulative mass arrival at each gridblock is an important variable in evaluating the potential locations of high-radionuclide concentration and migration, which is defined as the cumulative mass of contaminant arriving at each gridblock over time, normalized by the total mass of the initially released tracer from the tracer-releasing horizon about 300 m below surface. The cumulative mass travel time is the tracer travel time from the tracer-releasing horizon to the water table, which represents a measure of the overall tracer transport. The parameter sensitivity analysis of the contaminant transport is conducted for the five random parameters, permeability, porosity, van Genuchten α and n, and sorption coefficient (K_d) of the reactive tracer (^{237}Np).

For the case of independent parameters, Fig. 5 depicts the mean and standard deviation of $SRRC^2$ of the five random input parameters for the normalized cumulative mass arrival uncertainty of ^{237}Np after 1,000,000 years in the layers below the tracer-releasing horizon. The mean $SRRC^2$ values of the permeability are the largest in most layers. As noted earlier that the permeability also contributes the most to flow uncertainty, the results illustrate that the flow uncertainty also translates to uncertainty in tracer transport. The K_d of ^{237}Np has the second largest contributions to the tracer transport uncertainty in the layers with zeolitic and devitrified tuffs but is the smallest in the layers with vitric tuff (the geological information with corresponding tuffs is referred to Fig. 1, and BSC, 2004b). The reason is that uncertainty of K_d is relatively small for vitric tuff and large for zeolitic and devitrified tuffs (BSC, 2004b). In general, the parameter uncertainty in permeability contributes about 30% to the tracer transport uncertainties for the layers, and the contributions of other parameters vary with layers from close to zero to about 20%, Fig. 5b depicts the relative large standard deviation of $SRRC^2$ values for the parameters, indicating large variability of $SRRC^2$ within each layer.

Fig. 6 shows the $SRRC^2$ values of the five independent parameters for travel time uncertainty of ^{237}Np. At early stage, the permeability and the van Genuchten α have more contributions to the uncertainty in overall tracer transport, the same sensitivity results as the flow simulation. This observation may be explained in part

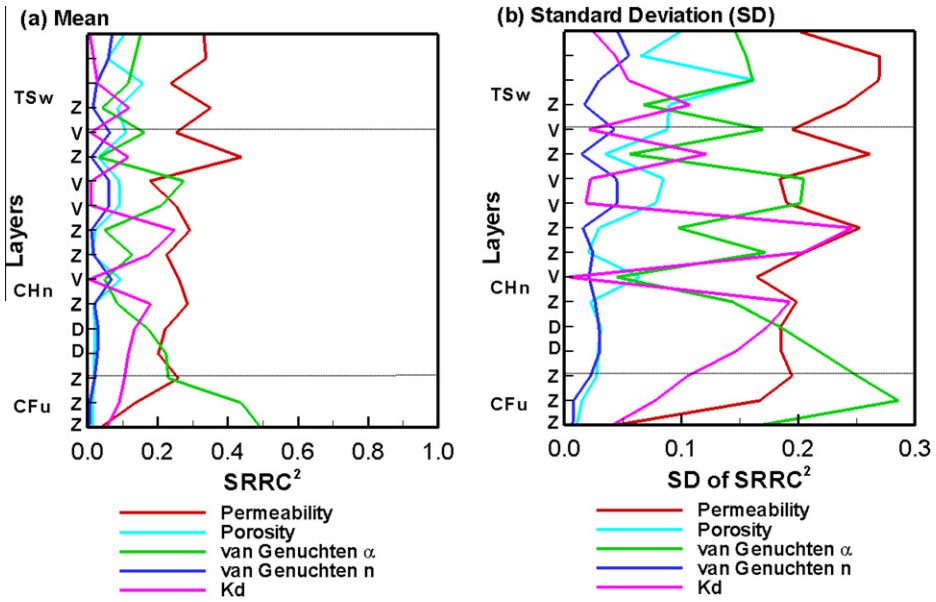

Fig. 5. The mean and standard deviation of standardized rank regression coefficient ($SRRC^2$) of permeability, porosity, van Genuchten α, and n, and sorption coefficient (Kd) on normalized cumulative mass arrival uncertainty of ^{237}Np after 1,000,000 years in the layers below the tracer-releasing horizon (Z – zeolitic tuff; V – vitric tuff; D – devitrified tuff).

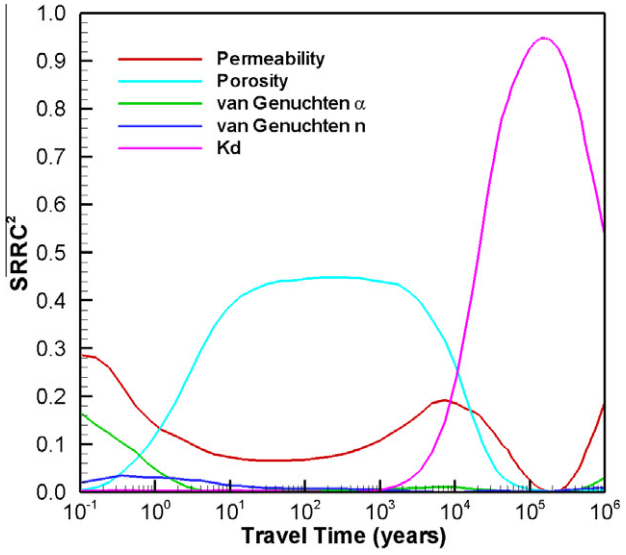

Fig. 6. The standarized rank regression coefficent ($SRRC^2$) of permeability, porosity, van Genuchten α and n, and Kd on travel time uncertainty of ^{237}Np.

by the fact that early arrival of the tracer at the water table is mainly along the faster flow paths. As time evolves, the porosity starts to make impact on the uncertainty in the overall tracer transport. After 10,000 years, the $SRRC^2$ values for the sorption coefficient are larger than those for the other parameters, indicating the sorption coefficient is the most important parameter on the overall tracer transport uncertainty after 10,000 years.

For the case of the correlated parameters, Fig. 7 shows the mean values of the uncorrelated, correlated, and total sensitivity indices, S, for permeability, porosity, van Genuchten α and n, and K_d on the normalized cumulative mass arrival uncertainty of ^{237}Np after 1000,000 years in the layers below the tracer-releasing horizon. The mean values of uncorrelated S (Fig. 7a) show that the permeability has the largest contributions on transport uncertainty in most layers, which is similar to the results with the independent parameters. Fig. 7b of the correlated S values shows that the mean values of correlated S for permeability and van Genuchten α are almost the same as those for porosity and van Genuchten n, respectively. The partial variances contributed by the correlated parameters to transport uncertainty have the same trends as the values of the parameter correlations. The mean values of correlated S are zero for K_d in all layers, because the parameter is not correlated with other input parameters for this study. The mean values of total S (Fig. 7c) are used to rank the relative importance of the parameters for each layer. The permeability is the most important parameter with around 20% contributions to the transport uncertainty for most layers. The relative importance for other parameters varies in a range of 0–20% contributions to transport uncertainty for different layers. The parameter uncertainty in K_d has the second largest contributions to transport uncertainty in the layers of devitrified and zeolitic tuffs and the smallest ones in the layers of vitric tuff, which are the same as the results without considering parameter correlations.

Fig. 8 shows the total, uncorrelated, and correlated S for the five correlated uncertain parameters on the travel time uncertainty of ^{237}Np. At the early stage, the van Genuchten α and n parameters have the largest total S on overall tracer transport uncertainty due to their large partial variances contributed by correlated variances of the parameters. As time evolves, both porosity and permeability become the most important parameters and the van Genuchten α and n parameters become insignificant. The sorption coefficient becomes the dominant parameter on the uncertainty of overall tracer transport at the water table after 10,000 years.

Fig. 7b depicts relatively large mean values of correlated S for the parameters in several layers, due to the high parameter correlations in these layers (Figs. 4b and 7b). It indicates that the partial variances contributed by the correlated parameters largely depend on the values of their correlations. The comparison of sensitivity analysis results with (Fig. 7c) and without (Fig. 5a) parameter correlations shows the parameter K_d has the same contributions for both cases, because K_d is uncorrelated with other parameters. The contributions of van Genuchten n significantly increase with the decreased importance of van Genuchten α after the parameter correlations are taken into account, while the importance of

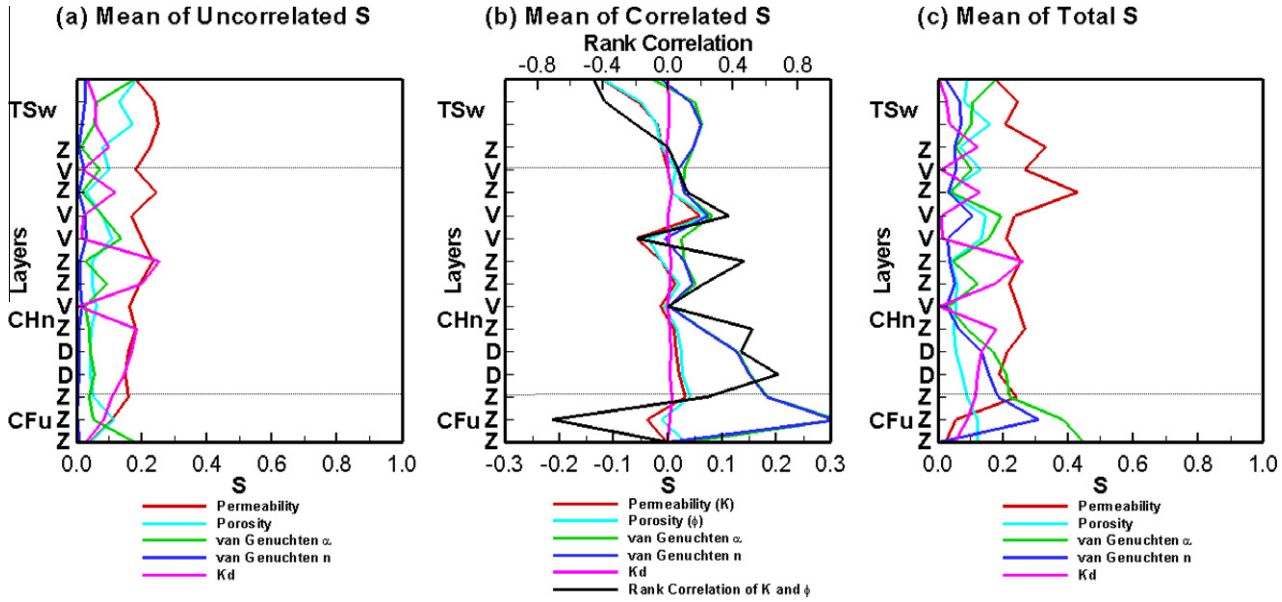

Fig. 7. The sensitivity indices (S) of permeability, porosity, van Genuchten α, and n, and Kd in the layers below the tracer-releasing horizon (Z – zeolitic tuff; V – vitric tuff; D – devitrified tuff).

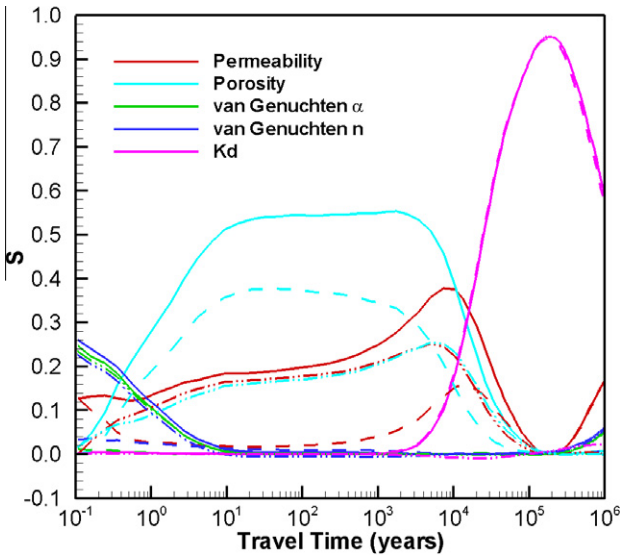

Fig. 8. The total (solid line), uncorrelated (dash line), and correlated (dashdot line) sensitivity indices (S) of permeability, porosity, van Genuchten α and n, and Kd on travel time uncertainty of ^{237}Np.

porosity slightly increases with the slightly decreased contributions of permeability to the transport uncertainty. This is due to the large correlations between van Genuchten α and n (Fig. 4b) and relatively small correlations between permeability and porosity (Fig. 7b) in most layers.

The permeability and the van Genuchten α are the two most important parameters on the travel time uncertainty at the water table at early stage, when the parameter correlations are not considered (Fig. 6). However, the van Genuchten n parameter becomes more important than the other parameters when the parameter correlations are considered (Fig. 8), due to large contributions from the correlated partial variances (Fig. 7). The parameter importance for the overall tracer transport uncertainty has the same rankings at the early stage. However, the correlated contributions for permeability and porosity account for large portions of their total partial variances, when the parameter correlations are considered. It indicates that the effects of parameter correlations, as an important factor for sensitivity in results, should be considered in uncertainty analysis.

4. Conclusions

The sample-based regression and decomposition methods are used for evaluating the sensitivity of the unsaturated flow and contaminant transport uncertainties with and without considering parameter correlations. This study not only gives the ranks of parameter importance on flow and transport uncertainties but also apportions the contributions of individual input parameters to the output uncertainties.

When the input parameters are independent, the uncertainties in the permeability and van Genuchten α are the major contributors to the flow uncertainty. For the tracer transport uncertainty, the uncertainties in permeability and van Genuchten α also have the most important contributions to the uncertainty in total cumulative mass arrival at the water table at the early stage. As time evolves, the uncertainty in porosity became more important. As the transport progresses further, the sorption coefficient of the reactive tracer becomes the dominant parameter in contributing to the uncertainty in overall tracer transport. The contribution of van Genuchten n to the flow and transport uncertainties is limited.

When the input parameters are correlated, the uncertainty in van Genuchten n has more contribution to the flow uncertainty, mainly due to its correlation with the van Genuchten α. The van Genuchten n and porosity also become more important on the transport uncertainty when the parameter correlations are considered due to their correlations with the van Genuchten α and permeability, respectively. The importance of sorption coefficient to the tracer transport uncertainty does not change when the parameter correlations are considered, since no correlations between the sorption coefficient and other hydraulic parameters are considered in this study. Therefore, this study illustrated that the parameter correlations have significant effects on the sensitivity and uncertainty analysis of unsaturated flow and contaminant transport.

To our best knowledge, this is the first time that sample-based regression and decomposition methods are applied to complex hydrogeologic systems such as the unsaturated zone at Yucca Mountain. In particular, the contributions of input parameter uncertainties to the flow and transport uncertainties are investigated for each hydrogeologic layer of the system and the parameter correlation is also incorporated into the sensitivity analysis to investigate its effect in each layer. The findings of this study are expected to be useful for uncertainty and sensitivity analysis of complex subsurface systems.

Acknowledgements

The first author was supported by the Maki Fellowship while he was at the Desert Research Institute, Nevada, USA. This study was also supported by the US Department of Energy (DOE) under the co-operative agreement between DOE and the Nevada System of Higher Education, and the Applied Research Initiative of Nevada Grant # 06HQGR0098. The third author was supported in part by the ORAU/ORNL High Performance Computing (HPC) Grant Program.

Appendix A

This appendix briefly describes the numerical model (EOS9 and T2R3D modules of TOUGH2 code), model domain, model input parameters, site measurements and variations of the parameters used in this study. For more details, readers are referred to Wu et al. (2004, 2007), Wu and Pruess (2000), BSC (2004a,b), Ye et al. (2007), and Pan et al. (2009b).

A.1. Governing equations of UZ numerical model

A 3-D site-scale numerical model was developed to simulate the flow and transport of three mass components (air, water, and tracer) in the UZ of YM. Since the dual-continuum approach is used, a doublet of governing equations of flow and transport are used to simulate fluid flow, chemical transport, and heat transfer processes in the two-phase (air and water) system of fractured rock for fracture and matrix, respectively. The physical processes of unsaturated flow in fracture and matrix are governed by Richards' equation, conservation of mass, and Darcy's law (BSC, 2004a; Wu and Pruess, 2000).

The mass flux in matrix or fracture (F^k) can be calculated by Darcy's law (BSC, 2004a; Wu and Pruess, 2000):

$$F^k = \sum_\beta X^k_\beta F_\beta; \quad F_\beta = \rho_\beta v_\beta = -k\frac{k_{r\beta}\rho_\beta}{\mu_\beta}(\nabla P_\beta - \rho_\beta g) \tag{A.1}$$

where β is fluid phase (liquid (L) or gas (G)); X^k_β is mass fraction of component k in phase β; F_β is mass flux in phase β; ρ_β is the density of phase β; v_β is the Darcy velocity; k is absolute permeability; $k_{r\beta}$ is relative permeability; μ_β is viscosity; g is gravity acceleration constant; and P_β is capillary pressure.

The Richards' equation can be described as (BSC, 2004a):

$$\frac{\partial}{\partial t}\theta_\beta = div[K_\beta \nabla \psi_\beta] + q_\beta \tag{A.2}$$

where $\theta_\beta = \phi S_\beta$ is specific volumetric moisture content for fracture or matrix (ϕ is porosity and S_β is the saturation of phase β); $K_\beta = k k_{r\beta}\rho_\beta g/\mu_\beta$ is hydraulic conductivity with $k_{r\beta}$ being the relative permeability, $\psi_\beta = z + P_\beta/(\rho_\beta g)$ is the total water potential with z being elevation, and q_β is sinks and sources.

The van Genuchten model is used to estimate water capillary pressure and unsaturated hydraulic conductivity for matrix and fracture continuums. The relationship between water content (θ) of a porous medium and capillary pressure is (van Genuchten, 1980):

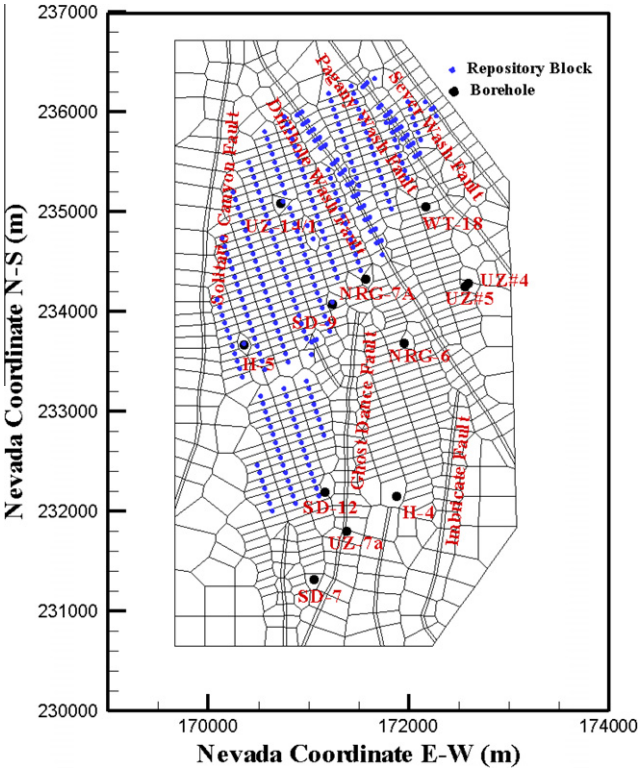

Fig. A.1. Plan view of the 3-D UZ numerical model grid showing the model domain, faults, high-level radioactive waste repository layout, and locations of several boreholes (modified from BSC, 2004a). (For interpretation of the references to colour in this figure legend, the reader is referred to the web version of this article.)

$$h(\theta) = \left\{\left(\frac{\theta-\theta_r}{\theta_S-\theta_r}\right)^{\frac{n}{1-n}} - 1\right\}^{\frac{1}{n}} \Big/ \alpha \tag{A.3}$$

where $h(\theta)$ is capillary pressure head; α and n are water retention parameters related to water entry pressure and soil pore size distribution, respectively; θ_s and θ_r are saturated and residual volumetric water contents, respectively. The relationship between unsaturated hydraulic conductivity $k(\theta)$ and water content can be described as:

$$k(\theta) = k_S\left(\frac{\theta-\theta_r}{\theta_S-\theta_r}\right)^{0.5}\left\{1-\left[1-\left(\frac{\theta-\theta_r}{\theta_S-\theta_r}\right)^{\frac{n}{1-n}}\right]^{\frac{n-1}{n}}\right\}^2 \tag{A.4}$$

where k_S is saturated hydraulic conductivity.

The processes of tracer transport in UZ include advection, diffusion, and dispersion in heterogeneous porous media, which are governed by Fick's law and conservation of mass (Wu and Pruess, 2000). The mass flux (F^k) is the summation of mass flux by advection, F^k_A, and mass flux by diffusion and dispersion, F^k_D, i.e., (Wu and Pruess, 2000)

$$F^k = F^k_A + F^k_D \tag{A.5}$$

and F^k_A and F^k_D are calculated via

$$F^\kappa_A = \sum_\beta (X^k_\beta \rho_\beta v_\beta) \tag{A.6}$$

$$F^\kappa_D = -\sum_\beta \left(\rho_\beta \underline{D}^k_\beta \cdot \nabla X^k_\beta\right) \tag{A.7}$$

where $\underline{D}^k_\beta$ is diffusion–dispersion tensor for both molecular diffusion and hydraulic dispersion for component k in phase β.

Table A.1
Descriptive statistics for matrix porosity and saturated hydraulic conductivity.

Major units	Layer name	Porosity (Φ)[c]					Saturated hydraulic conductivity (K_S, m/s)[c]					r[d]
		Mean	SD	Min	Max	N	Mean	SD	Min	Max	N	
TCw	CCR&CUC	0.241	0.073	0.038	0.431	124	5.80E−08	6.53E−08	2.03E−08	1.33E−07	3	e
	CUL&CW	0.088	0.032	0.032	0.213	694	7.68E−10	3.02E−09	2.15E−13	1.25E−08	17	−0.50
	CMW	0.200	0.055	0.1	0.452	96	1.89E−08	4.21E−08	3.34E−12	9.41E−08	5	0.60
PTn	CNW	0.387	0.069	0.228	0.633	104	2.90E−07	3.38E−07	5.12E−12	8.79E−07	10	0.61
	BT4	0.428	0.100	0.134	0.669	58	4.56E−06	7.59E−06	1.80E−10	2.54E−05	11	0.26
	TPY	0.233	0.057	0.073	0.309	39	1.38E−08	1.52E−08	3.00E−09	2.45E−08	2	e
	BT3	0.413	0.082	0.137	0.578	73	1.77E−06	2.03E−06	1.90E−09	7.30E−06	11	0.03
	TPP	0.498	0.041	0.388	0.623	159	1.17E−06	5.76E−07	9.00E−08	1.74E−06	11	−0.47
	BT2	0.490	0.095	0.104	0.614	176	7.10E−06	6.87E−06	1.24E−09	2.06E−05	21	0.42
TSw	TC	0.054	0.036	0.012	0.273	75	3.21E−08	6.72E−08	1.70E−11	1.68E−07	6	−0.49
	TR	0.157	0.030	0.062	0.267	449	2.03E−07	1.37E−06	1.70E−11	9.37E−06	47	0.39
	TUL	0.155	0.030	0.076	0.25	438	3.94E−08	2.33E−07	4.20E−13	1.42E−06	37	0.40
	TMN	0.111	0.020	0.055	0.192	277	4.18E−11	1.72E−10	4.76E−13	1.23E−09	74	0.48
	TLL	0.131	0.031	0.088	0.263	502	4.11E−09	1.31E−08	1.39E−12	7.65E−08	52	−0.46
	TM2&TM1	0.103	0.025	0.053	0.341	300	4.28E−07	2.00E−06	5.33E−13	9.39E−06	22	−0.39
	PV3	0.043	0.040	0.011	0.34	125	1.66E−10	5.45E−10	8.63E−14	2.25E−09	17	−0.20
	PV2a	0.275	0.096	0.11	0.415	13	b	b	b	b	b	e
	PV2v	0.243	0.122	0.048	0.47	49	3.23E−06	3.69E−06	5.03E−11	1.20E−05	16	0.06
CHn	BT1a	0.285	0.051	0.158	0.4	46	1.90E−08	3.21E−08	1.83E−13	8.70E−08	10	0.12
	BT1v	0.324	0.085	0.031	0.5	80	3.76E−06	5.77E−06	1.04E−10	2.20E−05	35	0.37
	CHV	0.341	0.048	0.04	0.49	130	1.48E−05	1.89E−05	1.68E−12	7.20E−05	47	−0.19
	CHZ	0.322	0.048	0.099	0.433	520	1.19E−09	9.62E−09	3.88E−13	9.54E−08	99	0.47
	BTa	0.271	0.046	0.181	0.418	73	4.05E−11	6.96E−11	2.08E−13	2.10E−10	9	0.22
	BTv	a	a	a	a	a	b	b	b	b	b	e
	PP4	0.327	0.050	0.216	0.44	56	4.62E−08	1.08E−07	8.44E−13	3.08E−07	8	0.52
	PP3	0.318	0.032	0.246	0.395	168	6.91E−08	6.72E−08	4.20E−12	3.65E−07	51	0.45
	PP2	0.221	0.058	0.099	0.333	127	1.56E−09	3.01E−09	3.75E−12	1.15E−08	35	0.68
	PP1	0.297	0.043	0.164	0.426	280	9.63E−08	3.88E−07	1.70E−12	1.94E−06	28	0.24
CFu	BF3	0.142	0.075	0.059	0.369	105	1.31E−08	2.01E−08	6.90E−11	5.58E−08	7	−0.71
	BF2	0.234	0.049	0.16	0.329	40	b	b	b	b	b	e

Note: (a) Only one porosity data point is available for BTv. (b) Only one saturated conductivity data point is available for Pv2a, BTv and BF2 respectively. (c) SD is standard deviation of the sample; Min, Max are the minimum and maximum values of the sample; N is the sample size. (d) r is Spearman rank correlation coefficient between the porosity and saturated hydraulic conductivity. (e) The sample size is not sufficient to estimate the Spearman rank correlation.

A.2. Model domain, numerical grid and approach

The 3-D numerical model grid representing the UZ system consists of 980 mesh columns of both fracture and matrix continua along a horizon grid layer, and each column includes an average of 45 model layers representing the hydrogeologic layers (BSC, 2004a). Refined mesh is used near the potential repository and natural faults. Fig. A.1 shows the plan view of the 3-D numerical grid with the model domain, proposed repository layout, borehole location, and faults.

The ground surface and the water table are treated as the top and bottom model boundaries, where the pressure and saturation are specified as boundary conditions. The no-flux boundary condition is specified for the lateral boundaries. A present-day net infiltration estimate with a constant rate of 4.43 mm/year within the UZ model grid is applied as a source term to the fracture gridblocks within the second grid layer from the top of the domain, as the first layer is treated as a Dirichlet boundary to represent average atmospheric conditions on the land surface. The spatial distribution of the net infiltration over the domain can be referred to Fig. 2 in Ye et al. (2007). The initial condition is the steady-state flow field of a previous run with a similar modeling condition. The transient-state transport simulation is conducted for 1,000,000 years. At the start time of simulation, constant concentration source is instantaneously released from the fracture continuum gridblocks (blue points in Fig. A.1) representing the once proposed repository (BSC, 2004a). The transport model shares the same boundaries as the flow model, with zero concentration at the top and bottom boundaries and no-flux lateral boundary conditions.

The integral finite-difference method is used to discretize the governing equations in Space. Time is discretized as a first-order finite difference associated with the numerical solution (Pruess et al., 1999; Wu and Pruess, 2000). The time increment is automatically adjusted at each time level according that if the convergence can be reached within a certain number of iterations. If no convergence can be reached within the iterations, the new reduced time step size is set to start a new iteration process. The initial time step size is 10^5 s in this study. The computational time varies from 2 to 10 h for different flow simulations with varied model input parameters. The steady-state flow fields can be examined by the mass balance (i.e., equivalent inflow and outflow) over the entire flow domain.

A.3. Model input parameters

Because of the dual-continuum approach, two sets of hydraulic and transport properties and other intrinsic properties are needed for the fractured and matrix continua. The basic parameters used for each model layer include (a) fracture properties (frequency, spacing, porosity, permeability, van Genuchten α and n parameters, residual saturation, and fracture–matrix interface area); (b) matrix properties (porosity, permeability, van Genuchten α and n parameters, and residual saturation); (c) transport properties (grain density, diffusion, adsorption, and tortuosity coefficients); and (d) fault properties (porosity, matrix and fracture permeability, and active fracture–matrix interface area).

This study treats matrix permeability, porosity, van Genuchten α and n parameters, and sorption coefficient of reactive tracer as

Table A.2
The estimates of mean and standard deviation of van Genuchten α (1/bar) and m parameters.

Major units	Layer name	Sample size	$\mu_{\log(\alpha)}$	$\sigma_{\log(\alpha)}$	μ_m	σ_m	r
TCw	CCR&CUC	3	0.004	0.244	0.388	0.081	−0.958
	CUL&CW	10	−0.509	0.199	0.280	0.046	−0.897
	CMW	6	−0.488	0.192	0.259	0.044	−0.886
PTn	CNW	8	1.207	0.269	0.245	0.038	−0.862
	BT4	8	1.164	0.169	0.219	0.019	−0.882
	TPY	2	0.391	0.728	0.247	0.104	−0.941
	BT3	3	1.897	0.375	0.182	0.028	−0.899
	TPP	3	1.015	0.189	0.300	0.039	−0.861
	BT2	11	1.992	0.335	0.126	0.017	−0.915
TSw	TC	4	0.939	0.544	0.218	0.068	−0.870
	TR	5	0.055	0.118	0.290	0.025	−0.870
	TUL	4	−0.210	0.114	0.283	0.025	−0.894
	TMN	3	−0.074	0.776	0.317	0.122	−0.941
	TLL	5	0.032	0.447	0.216	0.058	−0.072
	TM2&TM1	3	−0.081	0.934	0.442	0.173	−0.825
	PV3	5	−0.206	0.446	0.286	0.092	−0.865
	PV2a	1	−0.337	0.156	0.059	0.007	−0.937
	PV2v	1	0.686	0.043	0.293	0.011	−0.831
CHn	BT1a	3	−1.678	0.183	0.349	0.073	−0.885
	BT1v	3	0.940	0.050	0.240	0.008	−0.854
	CHV	5	1.413	0.092	0.158	0.008	−0.492
	CHZ	4	−0.648	0.094	0.257	0.022	−0.879
	BTa	1	−1.807	0.043	0.499	0.036	−0.699
	BTv	1	0.196	0.253	0.147	0.025	−0.901
	PP4	3	−1.349	0.513	0.474	0.200	−0.881
	PP3	5	−0.055	0.094	0.407	0.033	−0.906
	PP2	3	−0.622	0.168	0.309	0.044	−0.884
	PP1	3	−1.036	0.442	0.272	0.116	−0.932
CFu	BF3	2	0.098	0.940	0.193	0.077	−0.909
	BF2	1	−1.921	0.032	0.617	0.070	−0.164

Note: μ is the mean values of the van Genuchten parameters; σ is standard deviation; r is Spearman rank correlation between the parameters.

random based on a sensitivity analysis of Zhang et al. (2006), which illustrated that flow and transport simulations are not sensitive to fracture properties because fracture flow dominates over the entire model domain. Other matrix parameters (e.g., residual saturation) are considered as deterministic in this study because of their small spatial variability in the study site.

A.4. Site measurements and variations of model input parameters

The random fields of the five random parameters are generated based on the site measurements and statistical methods. Based on core samples collected from 33 boreholes, 546 measurements of matrix saturated hydraulic conductivity (converted into permeability in this study) and 5257 measurements of porosity are obtained (Flint, 1998, 2003; BSC, 2003). Table A.1 lists the statistics of measured porosity and saturated hydraulic conductivity and their rank correlations. Measurements of parameters of the van Genuchten water retention equation are sparse within each hydrogeologic layer and there are only several samples available to estimate the water retention parameters (Flint, 1998; BSC, 2003). The probability density functions (PDFs) of water retention parameters (e.g., van Genuchten α and m) are estimated using a non-conventional maximum likelihood approach (Pan et al., 2009b). Their rank correlations are calculated using the generated 2000-realization water retention parameter random fields based on the estimated covariance matrix and the multivariate Gaussian PDFs (Pan et al., 2009b). The fitted mean and variance of van Genuchten α and m and their rank correlations are listed in Table A.2. Over 700 measurements of sorption coefficient (K_d) of the reactive tracer, ^{237}Np, are available for three types of rocks: devitrified, vitric, and zeolitic tuffs, which are the rock types in the hydrogeologic layers (BSC, 2004b).

References

Boateng, S., Cawlfield, J.D., 1999. Two-dimensional sensitivity analysis of contaminant transport in the unsaturated zone. Ground Water 37 (2), 185–193.

Boateng, S., 2007. Probabilistic unsaturated flow along the textural interface in three capillary barrier models. Journal of Environmental Engineering 133 (11), 1024–1031.

BSC (Bechtel SAIC Company), 2003. Analysis of Hydrologic Properties Data. Report MDL-NBS-HS-000014 REV00. Lawrence Berkeley National Laboratory, Berkeley, California and CRWMS M&O, Las Vegas, Nevada, USA.

BSC, 2004a. UZ Flow Models and Submodels. Report MDL-NBS-HS-000006 REV02. Lawrence Berkeley National Laboratory, Berkeley, California and CRWMS M&O, Las Vegas, Nevada, USA.

BSC (Bechtel SAIC Company), 2004b. Radionuclide Transport Models Under Ambient Conditions. Report MDL-NBS-HS-000008 REV02. Lawrence Berkeley National Laboratory, Berkeley, California and CRWMS M&O, Las Vegas, Nevada, USA.

Campolongo, F., Cariboni, J., Staltelli, A., 2007. An effective screening design for sensitivity analysis of large models. Environmental Modelling & Software 22 (10), 1509–1518.

Cukier, R.I., Fortuin, C.M., Schuler, K.E., Petschek, A.G., Schaibly, J.H., 1973. Study of the sensitivity of coupled reaction systems to uncertainties in rate coefficients: I. Theory. Journal of Chemical Physics 59 (8), 3873–3878.

Cukier, R.I., Levine, H.B., Schuler, K.E., 1978. Nonlinear sensitivity analysis of multiparameter model systems. Journal of Computational Physics 26, 1–42.

Fang, S., Gertner, G.Z., Anderson, A.A., 2004. Estimation of sensitivity coefficients of nonlinear model input parameters which have a multinormal distribution. Computer Physics Communications 157, 9–16.

Flint, L.E., 1998. Characterization of Hydrogeologic Units Using Matrix Properties, Yucca Mountain, Nevada. Water Resources Investigation Report 97-4243. US Geological Survey, Denver, Colorado, USA.

Flint, L.E., 2003. Physical and hydraulic properties of volcanic rocks from Yucca Mountain, Nevada. Water Resources Research 39 (5), 1–13.

Fox, G.A., Muñoz-Carpena, R., Sabbagh, G.J., 2010. Influence of flow concentration on parameter importance and prediction uncertainty of pesticide trapping by vegetative filter strips. Journal of Hydrology 384, 164–173.

Helton, J.C., 1993. Uncertainty and sensitivity analysis techniques for use in performance assessment for radioactive waste disposal. Reliability Engineering & System Safety 42, 327–367.

Helton, J.C., Johnson, J.D., Rollstin, J.A., Shiver, A.W., Sprung, J.L., 1995. Uncertainty and sensitivity analysis of chronic exposure results with the MACCS reactor accident consequence model. Reliability Engineering & System Safety 50 (2), 137–177.

Helton, J.C., Davis, F.J., 2002. Illustration of sampling-based methods for uncertainty and sensitivity analysis. Risk Analysis 22 (3), 591–622.
Helton, J.C., Davis, F.J., Johnson, J.D., 2005. A comparison of uncertainty and sensitivity analysis results obtained with random and Latin hypercube sampling. Reliability Engineering & System Safety 89, 305–330.
Helton, J.C., Johnson, J.D., Sallaberry, C.J., Storlie, C.B., 2006. Survey of sampling-based analysis. Reliability Engineering & System Safety 91, 1175–1209.
Illman, W.A., Hughson, D.L., 2005. Stochastic simulations of steady state unsaturated flow in a three-layer, heterogeneous, dual continuum model of fractured rock. Journal of Hydrology 307, 17–37.
Jacques, J., Lavergne, C., Devictor, N., 2006. Sensitivity analysis in presence of model uncertainty and correlated inputs. Reliability Engineering & System Safety 91, 1126–1134.
Lemke, L.D., Abriola, L.M., Lang, J.R., 2004. Influence of hydraulic property correlation on predicted dense nonaquesous phase liquid source zone architecture, mass recovery and contaminant flux. Water Resources Research 40, W12417. doi:10.1029/2004WR003061.
Li, B., Yeh, T.-C.J., 1998. Sensitivity and moment analyses of head in variably saturated regimes. Advances in Water Resources 21 (6), 477–485.
Lu, Y., Mohanty, S., 2001. Sensitivity analysis of a complex, proposed geologic waste disposal system using the Fourier amplitude sensitivity test method. Reliability Engineering & System Safety 72, 275–291.
Manache, G., Melching, C.S., 2008. Identification of reliable regression- and correlation-based sensitivity measures for importance ranking of water-quality model parameters. Environmental Modelling & Software 23, 549–562.
Mckay, M.D., 1997. Nonparametric variance-based methods of assessing uncertainty importance. Reliability Engineering & System Safety 57 (3), 267–279.
Mishra, S., Deeds, N.E., Ramarao, B.S., 2003. Application of classification trees in the sensitivity analysis of probabilistic model results. Reliability Engineering & System Safety 79, 123–129.
Mishra, S., 2009. Uncertainty and sensitivity analysis techniques for hydrologic modeling. Journal of Hydroinformatics 11 (3–4), 282–296.
Montazer, P., Wilson, W.E., 1984. Conceptual Hydrologic Model of Flow in the Unsaturated Zone, Yucca Mountain, Nevada. Water Resources Investigation Report 84-4345. US Geological Survey, Lakewood, Colorado, USA.
Mohanty, S., Wu, Y.-T., 2001. CDF sensitivity analysis technique for ranking influential parameters in the performance assessment of the proposed high-level waste repository at Yucca Mountain, Nevada, USA. Reliability Engineering & System Safety 73, 167–176.
Morris, M.D., 1991. Factorial sampling plans for preliminary computational experiments. Technometrics 33 (2), 161–174.
Muñoz-Carpena, R., Zajac, Z., Kuo, Y.-M., 2007. Evaluation of water quality models through global sensitivity and uncertainty analyses techniques: application to the vegetative filter strip model VFSMOD-W. Transactions of the ASABE 50 (5), 1719–1732.
Muñoz-Carpena, R., Fox, G., Sabbagh, G.J., 2010. Parameter importance and uncertainty in predicting runoff pesticide reduction with filter strips. Journal of Environmental Quality 39, 630–641.
Pan, F., Ye, M., Zhu, J., Wu, Y.S., Hu, B.X., Yu, Z., 2009a. Incorporating layer- and local-scale heterogeneities in numerical simulation of unsaturated flow and tracer transport. Journal of Contaminant Hydrology 103, 194–205. doi:10.1016/j.jconhyd.2008.10.012.
Pan, F., Ye, M., Zhu, J., Wu, Y.S., Hu, B.X., Yu, Z., 2009b. Numerical evaluation of uncertainty in water retention parameters and effect on predictive uncertainty. Vadose Zone Journal 8 (1), 158–166. doi:10.2136/vzj2008.0092.
Pohlmann, K.F., Hassan, A.E., Chapman, J.B., 2002. Modeling density-driven flow and radionuclide transport at an underground nuclear test: Uncertainty analysis and effect of parameter correlation. Water Resources Research 38 (5), 1059. doi:10.1029/2001WR001047.
Pruess, K., Oldenburg, C., Moridis, G., 1999. TOUGH2 User's Guide, Version 2.0. LBL-43134. Lawrence Berkeley Laboratory, Berkeley, California, USA.
Rojas, R., Feyen, L., Dassargues, A., 2009. Sensitivity analysis of prior model probabilities and the value of prior knowledge in the assessment of conceptual model uncertainty in groundwater modeling. Hydrological Processes 23, 1131–1146.
Saltelli, A., Marivoet, J., 1990. Non-parametric statistics in sensitivity analysis for model output: a comparison of selected techniques. Reliability Engineering & System Safety 28, 229–253.
Saltelli, A., Sobol, I.M., 1995. About the use of rank transformation in sensitivity analysis of model output. Reliability Engineering & System Safety 50, 225–239.
Saltelli, A., Tarantola, S., Chan, K., 1999. A quantitative model-independent method for global sensitivity analysis of model output. Technometrics 41 (1), 39–56.
Saltelli, A., Chan, K., Scott, E.M., 2000. Sensitivity Analysis. John Wiley & Sons, Chichester, UK.
Saltelli, A., Ratto, M., Tarantola, S., Campolongo, F., Commission, E.Joint Research Centre of Ispra, 2006. Sensitivity analysis practices: Strategies for model-based inference. Reliability Engineering & System Safety 91, 1109–1125.
Saltelli, A., Ratto, M., Andres, T., Campolongo, F., Cariboni, J., Gatelli, D., Saisana, M., Tarantola, S., 2008. Global Sensitivity Analysis: The Primer. John Wiley & Sons, Chichester, UK.
Sobol, I.M., 1993. Sensitivity estimates for nonlinear mathematical models. Mathematical Modeling & Computational Experiment 1 (4), 407–414.
Sobol, I.M., 2001. Global sensitivity indices for nonlinear mathematical models and their Monte Carlo estimates. Mathematics and Computers in Simulation 55, 271–280.
van Genuchten, M.Th., 1980. A closed-form equation for predicting the hydraulic conductivity of unsaturated soils. Soil Science Society of American Journal 44 (5), 892–898.
Winter, C.L., Guadagnini, A., Nychka, D., Tartakovsky, D.M., 2006. Multivariate sensitivity analysis of saturated flow through simulated highly heterogeneous groundwater aquifers. Journal of Computational Physics 217, 166–175.
Wu, Y.S., Ahlers, C.F., Fraser, P., Simmons, A., Pruess, K., 1996. Software qualification of Selected TOUGH2 Modules. LBNL-39490. Lawrence Berkeley Laboratory, Berkeley, California, USA.
Wu, Y.S., Pruess, K., 2000. Numerical simulation of non-isothermal multiphase tracer transport in heterogeneous fractured porous media. Advances in Water Resources 23, 699–723.
Wu, Y.S., Lu, G., Zhang, K., Bodvarsson, G.S., 2004. A mountain-scale model for characterizing unsaturated flow and transport in fractured tuffs of Yucca Mountain. Vadose Zone Journal 3, 796–805.
Wu, Y.S., Lu, G., Zhang, K., Pan, L., Bodvarsson, G.S., 2007. Analysis unsaturated flow patterns in fractured rock using an integrated modeling approach. Hydrogeology Journal 15, 553–572.
Xu, C., Gertner, G.Z., 2008. Uncertainty and sensitivity analysis for models with correlated parameters. Reliability Engineering & System Safety 93, 1562–1573.
Ye, M., Pan, F., Wu, Y.S., Hu, B.X., Shirley, C., Yu, Z., 2007. Assessment of radionuclide transport uncertainty in the unsaturated zone of Yucca Mountain. Advances in Water Resources 30, 118–134.
Zhang, K., Wu, Y.S., Houseworth, J.E., 2006. Sensitivity analysis of hydrological parameters in modeling flow and transport in the unsaturated zone of Yucca Mountain. Hydrogeology Journal 14, 1599–1619.
Zhou, Q., Liu, H.H., Bodvarsson, G.S., Oldenburg, C.M., 2003. Flow and transport in unsaturated fractured rock: effects of multiscale heterogeneity of hydrogeologic properties. Journal of Contaminant Hydrology 60, 1–30.
Zhu, J., Pohlmann, K.F., Chapman, J.B., Russell, C.E., Carroll, R.W.H., Shafer, D.S., 2010. Sensitivity of solute advective travel time to porosities of hydrogeologic units. Ground Water 48 (3), 442–447.